Nitrogen cycling on the Namibian shelf and slope over the last two climatic cycles: Local and global forcings

Laetitia Pichevin,[1] Philippe Martinez, Philippe Bertrand, Ralph Schneider, and Jacques Giraudeau

Département de Géologie et Océanographie, Université Bordeaux I, Université Mixte de Recherche-Centre National de la Recherche Scientifique, Talence, Cedex, France

Kay Emeis

Institute of Biogeochemistry and Marine Chemistry, University of Hamburg, Hamburg, Germany

Received 16 December 2003; revised 12 January 2005; accepted 17 February 2005; published 4 May 2005.

[1] In the light of new surface sediment $\delta^{15}N$ data collected over the Namibian shelf and slope, we examined glacial-interglacial variations of N inventory in the area of Lüderitz (25°6S) by deciphering $\delta^{15}N$ signals of three cores distributed from the upper to the lower continental slope. The lower slope cores display low $\delta^{15}N$ during cold periods and high $\delta^{15}N$ during climatic optima, akin to many other records from the world ocean, whereas the upper slope core displays a high-frequency low-amplitude $\delta^{15}N$ signal without obvious glacial-interglacial variability. This dissimilarity results from the segregation of the upwelling structure in two cells, decoupling nutrient dynamics of the shelf from those beyond the shelf-edge. The $\delta^{15}N$ signal of the coastal cell is relatively constant irrespective of wind strength variations and shows that nitrate was never depleted in the surface water. For the deeper cores, comparisons between N isotopic signals and indicators of paleoproductivity (total organic carbon) and upwelling intensity (sea surface temperature and dust grain size) reveal that, over Milankovitch cycles, nitrate delivery to the photic zone was driven by the nutrient richness of the South Atlantic Central Water (depending, in turn, on Aghulas water inflow and denitrification at a global scale) rather than by atmospheric forcing. We propose that the $\delta^{15}N$ signals of the deeper cores do not only mirror changes in relative nitrate utilization, as it seems the case over annual timescales, but are arguably influenced by global ocean changes in middepth nitrate $\delta^{15}N$.

Citation: Pichevin, L., P. Martinez, P. Bertrand, R. Schneider, J. Giraudeau, and K. Emeis (2005), Nitrogen cycling on the Namibian shelf and slope over the last two climatic cycles: Local and global forcings, *Paleoceanography*, *20*, PA2006, doi:10.1029/2004PA001001.

1. Introduction

[2] The Benguela upwelling system (BUS) is considered to have played a significant role as a carbon sink, especially since the closing of the Central American Isthmus, about 3 Myr ago [*Hay and Brock*, 1992]. The BUS is today the world's most productive eastern boundary current [*Carr*, 2002]. Whether local productivity in the past was mainly new production or related to processes of nutrient recycling is a tricky issue. Solving this question is, however, an essential prerequisite for estimates of the net CO_2 pumping attributable to this upwelling through the past and, ultimately, for forecasts of the future climate changes. In this regard, the mechanisms that control the local nutrient budget (nutrient loss, supply, utilization and recycling) and their variations with climate changes must be addressed. To date, only a few studies deal with cross-shore distribution of nutrients in the surface water of the modern BUS [*Dittmar and Birkicht*, 2001; *Tyrell and Lucas*, 2002; *Holmes et al.*, 2002]. Fewer still are those which attempt to reconstruct past variations of the surface nutrient inventory [*Holmes et al.*, 1999] from nearshore to offshore locations [*Lavik*, 2001].

[3] In this study, we intend to untangle the $\delta^{15}N$ signals of three sediment cores distributed from the upper to the lower continental slope off Namibia in order to assess changes in marine nitrogen inventory during the last 240 kyr. In the ensuing discussion, we use lithogenic grain size distribution and sea surface temperatures (SSTs) records as additional proxies for wind strength and upwelling intensity, respectively, and total organic carbon (TOC) and organic carbon accumulation rates (MARCorg) values as paleoproductivity indicators. Sediment core records are interpreted in the light of new $\delta^{15}N$ measurements from surface sediments which give insights into processes governing N cycling in the modern BUS.

2. Fate of Marine Nitrogen and the $\delta^{15}N$ Signal

[4] The $\delta^{15}N$ of the global nitrate pool averages 5‰ [*Sigman et al.*, 1997]. This value represents the balance

[1] Now at Centre Européen de Recherche et d'Enseignement des Géosciences de l'Environnement, Europole Méditerranéen de l'Arbois, Aix en Provence, France.

0883-8305/05/2004PA001001

between inputs and sinks of marine nitrogen at a global scale, namely river supply, N_2 fixation, burial (following biological utilization) and denitrification [*Brandes and Devol*, 2002]. Fixation of atmospheric nitrogen by diazotrophic primary producers does not involve observable fractionation and $\delta^{15}N$ of the fixed nitrogen is close to 0‰ [*Brandes et al.*, 1998]. Meanwhile, in the near absence of oxygen, water column denitrification transforms available nitrogen species to gaseous products, strongly discriminating against ^{15}N. As a result, in areas adjoining oxygen minimum zones (OMZs) in the equatorial and eastern tropical North Pacific (ETNP) and equatorial and eastern tropical South Pacific (ETSP) and the Indian Ocean, very high $\delta^{15}N_{NO3-}$ values are measured [*Brandes et al.*, 1998, *Ganeshram et al.*, 2000].

[5] Although N fixation can support productivity in some areas, new production is mainly sustained by advection or upwelling of new nitrate to the photic zone. During phytoplankton blooms, nitrate uptake is accompanied by fractionation that leads to an enrichment of the organic product in ^{14}N. The phytoplankton biomass is thus depleted in ^{15}N by a factor of ε (fractionation factor) relative to the remaining nitrate pool which is symmetrically enriched in $^{15}N_{NO3-}$ approximated by first-order Rayleigh fractionation kinetics.

[6] As the nutrient-rich water is advected offshore, the available nitrate pool becomes progressively consumed by producers and its isotopic composition shows increasing $\delta^{15}N$ values. As a result, producers growing on the residual pool will incorporate a greater proportion of ^{15}N than producers directly growing in the upwelled source waters. Thus, for a given starting pool of nitrate, a larger degree of relative nutrient utilization will produce an enrichment of sedimentary $\delta^{15}N$ [*Wada*, 1980; *Mariotti et al.*, 1982; *Altabet and François*, 1994; *Martinez et al.*, 2000]. Nevertheless, many other biochemical mechanisms can affect the $\delta^{15}N$ signal, i.e., nitrogen transfer through trophic levels [*Minagawa and Wada*, 1984; *Montoya and McCarthy*, 1995], relative abundance of terrestrial and marine organic matter (OM) [*Sweeney and Kapland*, 1980], OM decay in the water column and during early diagenesis [e.g., *Altabet*, 1991; *Francois et al.*, 1993; *Freudenthal et al.*, 2001; *Lehmann et al.*, 2003].

3. Methods

3.1. Samples and Stratigraphy

[7] The transect studied was recovered in 1996 on the R/V *Marion Dufresne* during the NAUSICAA cruise. The core MD962086 (25.81°S, 12.13°E) is located at 3606 m water depth and MD962098 (25.59°S, 12.63°E) at 2909 m water depth, both on the lower slope. MD962087 (25.6°S, 13.38°E) lies under 1029 m water depth, on the upper slope.

[8] The stratigraphies for MD962086 and 98 are based on oxygen isotope analyses of the benthic foraminifera *Cibicidoides wuellerstorfi* [*Bertrand et al.*, 2000]. These records were correlated with the normalized SPECMAP standard record [*Imbrie et al.*, 1984]. MD962087 stratigraphy for the last 40 kyr was given by seven AMS 14C dates (Table 1) determined on mixed planktic foraminifers [*Pichevin et al.*, 2004]. A 400-year reservoir correction was applied and dates were converted into calendar ages by using the Calib 4.3 program [*Stuiver et al.*, 1998]. As previously described in the work of *Pichevin et al.* [2004], the age model for the oldest part of the core results from the correlation between TOC and CaCO3 records of MD962087 and those of MD962098, MD962086 and between SSTs of MD962087 and GEOB 1712-4 (off Walvis Bay, 998 m water depth) published in the work of *Kirst et al.* [1999]. Surface sediments were collected in spring 2004 with the R/V *Alexander von Humbold* (K. Emeis, unpublished data, 2004).

3.2. Experiment

[9] The nitrogen content and isotopic composition of MD962098 and 87 was analyzed on bulk sediment samples with a Micromass mass spectrometer at the DGO (University of Bordeaux). For MD962086, N isotopes were measured at the University of British Columbia (by Tom Pedersen) with a Finnigan delta plus mass spectrometer and some samples were also analyzed in Bordeaux to ensure comparability, which was found to be within ±0, 2‰. The $\delta^{15}N$ and TOC measurements were performed at average sampling intervals of 1 kyr. Apparent relative nitrate utilization was estimated for the deep cores assuming first-order fractionation kinetics, and by deriving the equation of *Altabet and Francois* [1994]:

$$\delta^{15}NO^{-}_{3(f)} = \delta 15NO^{-}_{3(f=1)} - \varepsilon \times \ln(f) \quad (1)$$

$$\delta^{15}Nsed_{(f)} = \delta^{15}NO^{-}_{3(f)} - \varepsilon, \quad (2)$$

where F is the fraction of unutilized, remaining nitrate, $\delta^{15}NO^{-}_{3(f=1)}$ is the isotopic value of initial nitrate (5, 5‰), $\delta^{15}NO^{-}_{3(f)}$ is the isotopic value of remaining nitrate and $\delta^{15}Nsed_{(f)}$ is the isotopic value of sedimentary N (instantaneous product). We chose a fractionation coefficient of 5‰, based on recent observations [*Holmes et al.*, 1998].

[10] N isotopic signals of surface sediments were measured in the Institute of Biogeochemistry and Marine Chemistry, University of Hamburg (K. Emeis, unpublished data, 2004).

[11] TOC (wt%) was measured by elemental analyses (LECO). The mass accumulation rate of organic carbon (MARCorg) was calculated as following:

$$\mathrm{MARCorg}\left(\mathrm{g\ cm^{-2}\ kyr^{-1}}\right) = \mathrm{TOC(wt\%)} \times \mathrm{SR}\left(\mathrm{cm\ kyr^{-1}}\right) \times \mathrm{DBD}\ \left(\mathrm{g\ cm^{-3}}\right)/100, \quad (3)$$

where SR is the sedimentation rate calculated between two identified isotopic events or radio carbon dates and DBD is the dry bulk density based on the MST signals measured on board the *Marion Dufresne*.

[12] The SSTs estimates are based on alkenone measurements. Long-chain unsaturated ketones were extracted and analyzed by gas chromatography (J. Villanueva, unpublished data, 1999) following the methodology described in the work of *Villanueva and Grimalt* [1997]. The U^{K}_{37} values

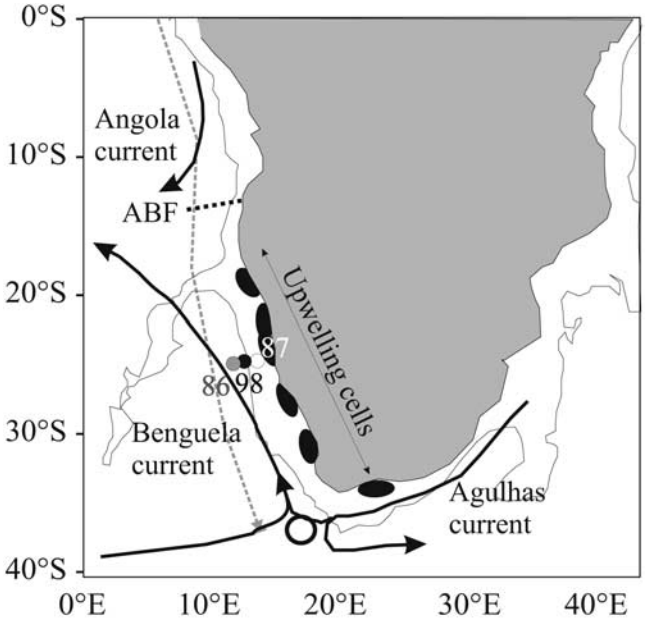

Figure 1. Schematic surface circulation around South Africa and core sites MD9720 86 (3606 m), 98 (2909 m), and 87(1028 m water depth). Profiles shown in Figure 3 are represented by a gray dashed line. The black line indicates the 400 m isobath. ABF, Angola Benguela Front.

were converted into temperatures by applying the equation of *Prahl et al.* [1988]. SSTs were estimated with a resolution of 1 to 10 kyr depending on the core and the time slice.

[13] Grain size analyses were performed on the lithogenic fraction of MD962087. Sampling interval is 700 years on average. In order to isolate the terrigenous inorganic material, carbonates, OM and biosilica were successively removed by using HCl (at 20°C), H_2O_2 (30% at 50°C during 3 to 4 days) and NaOH (30% at 80°C for 6–8 hours). Microscopic observations of smear slides showed that the biogenic constituents were properly removed by the chemical treatment. The grain size distribution of the remainder was measured with a Laser Malvern Mastersizer [*Pichevin et al.*, 2005].

4. Today's Water Mass and Nutrient Dynamics

4.1. Setting

[14] The modern upwelling system related to the Benguela coastal current (BCC) has been extensively described in the literature [e.g., *Lutjeharms and Meeuwis*, 1987; *Peterson and Stramma*, 1991; *Shannon and Nelson*, 1996; *Giraudeau et al.*, 2000]. Among the seven upwelling cells distributed along the southwestern African coast, the Lüderitz cell is noteworthy due to its central location (Figure 1). The southeastern trade (SET) winds, resulting from the pressure gradient between the Intertropical Convergent Zone (ITCZ), and the South Atlantic anticyclone are perennially consistent between 22 and 27°S. This allows permanent activity of the Lüderitz cell throughout the year. SET winds presently exert their maximal stress on the surface ocean in the area of Lüderitz [*Lutjeharms and Meeuwis*, 1987; *Summerhayes et al.*, 1995]. In addition, the broad Orange River shelf located around 29°S drives the coastal water flow northward along the isobaths. At the apex of the Orange River shelf (28°S), the topographical control ceases and the water is able to move cross-shore [*Largier and Boyd*, 2001]. These atmospheric and bathymetric conditions enable the formation of a highly productive, filamentous mixing domain streaming up to several hundreds of kilometers offshore Lüderitz.

4.2. Relative Nitrate Utilization in the Modern BUS

[15] Nitrate concentration in emerging waters off Lüderitz is often greater than 30 μM [*Tyrrell and Lucas*, 2002; *Dittmar and Birkicht*, 2001; *Conkright et al.*, 1998]. As the water is advected offshore, NO_3^{2-} fuels primary production and is intensively consumed. Yet, nitrate concentration in near surface ocean may remain >5 μM well after the shelf break [*Conkright et al.*, 1998]. *Holmes et al.* [2003] found nitrogen isotope ratios ranging from 5 to 12‰ in the surface sediments off Namibia. Sedimentary $\delta^{15}N$ variations are negatively correlated with near surface nitrate concentrations measured by *Conkright et al.* [1998]: nearshore locations usually show low sedimentary $\delta^{15}N$ corresponding to high $[NO_3^{2-}]$ in the surface waters. Sedimentary nitrogen isotope signal increases with the distance to the coast as $[NO_3^{2-}]$ diminishes, suggesting that relative nitrate utilization controls $\delta^{15}N$ on the Namibian slope [*Holmes et al.*, 2003]. In addition, seasonal variations of upwelling-driven SST has proved to be faithfully followed by changes in the $\delta^{15}N$ of sinking particles collected at 599 m water depth off Walvis Bay (22°S) [*Holmes et al.*, 1998, 2002, 2003]. When SSTs are low (November–December), primary production increases (as seen by high fluxes) due to enhanced nutrient supply to the surface, and the $\delta^{15}N$ signal is minimum and close to that of newly upwelled nitrate (5‰) [*Holmes et al.*, 1998, 2003].

[16] Our data supports the aforementioned results and interpretations concerning the Namibian slope. The distribution of surface sediment $\delta^{15}N$ (mapped on Figure 2) was extrapolated from more than fifty measurements scattered on the Namibian shelf and slope. For comparison, we estimated relative nitrate utilization in the surface waters using the Levitus 1994 database (http://ingrid.ldeo.columbia.edu/) and by subtracting annually averaged surface $[NO_3^{2-}]$ from 200 m water depth $[NO_3^{2-}]$. The result is shown on Figure 2. Disregarding the inner shelf, where precise $[NO^3]$ values do not exist, spatial distributions of both sedimentary $\delta^{15}N$ and calculated relative nitrate utilization agree well. Surface nitrate utilization and sedimentary $\delta^{15}N$ increase in tandem when surface [NO3] decreases with the distance to the coastal upwelling cells which draw new nitrate from below. Nitrate utilization values (f) and corresponding $\delta^{15}N$ ratios follow reasonably well the equation (2) derived from of *Altabet and Francois* [1994] and adapted for the Benguela region (r^2 = 0, 69). This tends to show that N isotope ratio witnesses relative nitrate utilization in the modern BUS. Additionally, the presence of a poleward under-current bringing nitrate-rich water from the Angola region explains increasing $[NO_3^{2-}]$ values toward the north

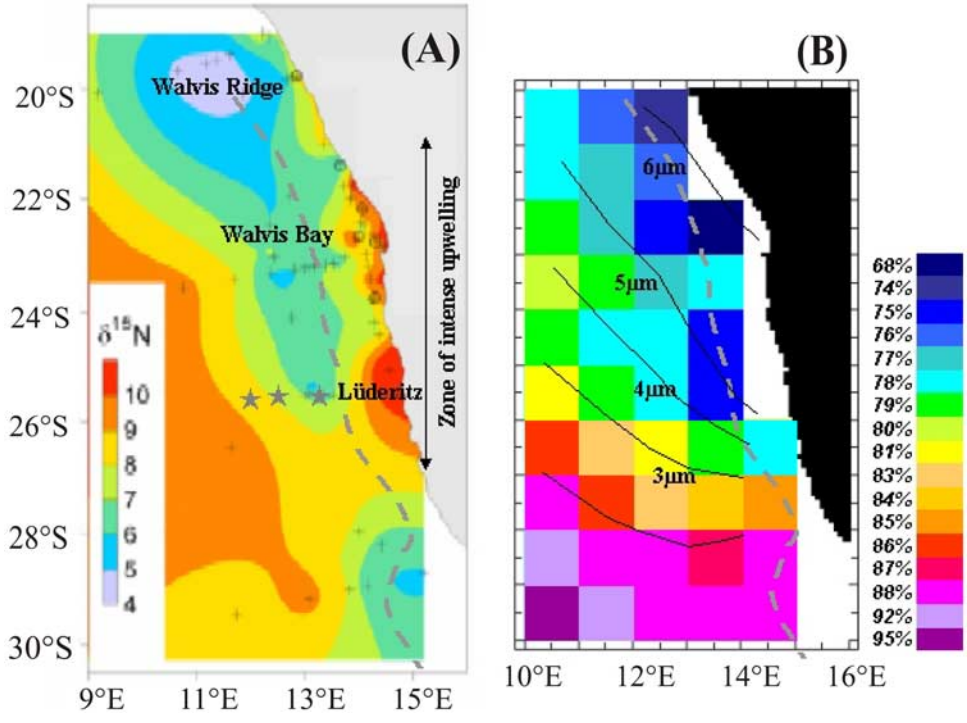

Figure 2. (a) Surface sediment $\delta^{15}N$ (‰) compared with (b) surface NO_3 isoconcentrations (µm L^{-1}, black lines) and estimates of relative nitrate utilization (%) calculated after Levitus database (http://ingrid.ldeo.columbia.edu/). Gray dashed line indicates the shelf break.

at 200 m water depth (not shown) and low sedimentary $\delta^{15}N$ values north of Lüderitz (Figure 2a).

[17] On the shelf, areas of very high sedimentary $\delta^{15}N$ (>9–10‰) are observed, especially where intense upwellings develop, between Walvis Bay and the Orange River mouth (Figure 2). Two explanations are suggested and discussed later on: (1) the advection of a coastal current carrying heavy nitrate from southern or northern locations or (2) the occurrence of water column denitrification over the shelf.

4.3. Denitrification on the Namibian Shelf?

[18] Water masses filling the southeastern Atlantic basin are shown in Figure 3. The high oxygen saturation of these water masses allows the whole water column to be well ventilated, and theoretically precludes the formation of an oxygen minimum zone (OMZ) in the region. However, rapid fluxes of OM, comparable to those supplying the Namibian slope and shelf, can lead to high oxidant demand, hence, to the establishment of hypoxic to sulfidic conditions in the sediment [*Morse and Emeis*, 1992; *Schulz et al.*, 1994; *Pichevin et al.*, 2004] and, arguably, in the overlying waters. In addition, oxygen depleted waters (<1 mL L^{-1}) are sporadically found at around 300–400 m water depth off Walvis Bay and Lüderitz shelf breaks [*Chapman and Shannon*, 1987; *Lass et al.*, 2000; *Mohrolz et al.*, 2001]. Formation of these oxygen deficient waters has been partly ascribed to local productivity, driving oxygen consumption, but also to southward intrusion of a poleward undercurrent emanating from the Angola gyre (Figure 3) [*Lass et al.*, 2000; *Mohrolz et al.*, 2001]. Because the circulation loop of surface and central currents is almost closed in the Angola dome, waters have a long residence time and are depleted in oxygen below the thermocline. This poleward undercurrent has been observed as far as 22°S and 27°S [*Gordon et al.*, 1995]. During intrusions of the poleward undercurrent, the BUS waters may sporadically behave as an OMZ, without reaching the critical concentration of 2 µM $O_2.L^{-1}$ required to start denitrification. However, blooms and subsequent respiration of the abundant settling OM may yield to water oxygen exhaustion and cause water column denitrification.

[19] Indeed, *Dittmar and Birkicht* [2001] and *Tyrrell and Lucas* [2002] reported nitrogen deficits (based on comparisons of nitrate and phosphate data, N:P-Redfield ratio) in the waters surrounding the Namibian shelf. They both attributed these losses to sedimentary and water column denitrification. Sedimentary denitrification implies no isotope effect [*Brandes and Devol*, 1997; *Sigman et al.*, 2001, 2003]. The influence of a shallow current transporting heavy nitrates along the coast from Angola or southern Namibia is unlikely considering the patchy distribution pattern of high $\delta^{15}N$ (Figure 2), and has never been reported. Thus even sporadic events of water column denitrification over the inner shelf are assumed to be responsible for the enrichment in ^{15}N in the inner shelf sediments.

4.4. Two-Celled Structure of the Upwellings

[20] When upwelling develops over a broad shelf, its structure is often divided in two cells, nearshore and beyond the shelf break [*Smith*, 1995]. A two-celled circulation

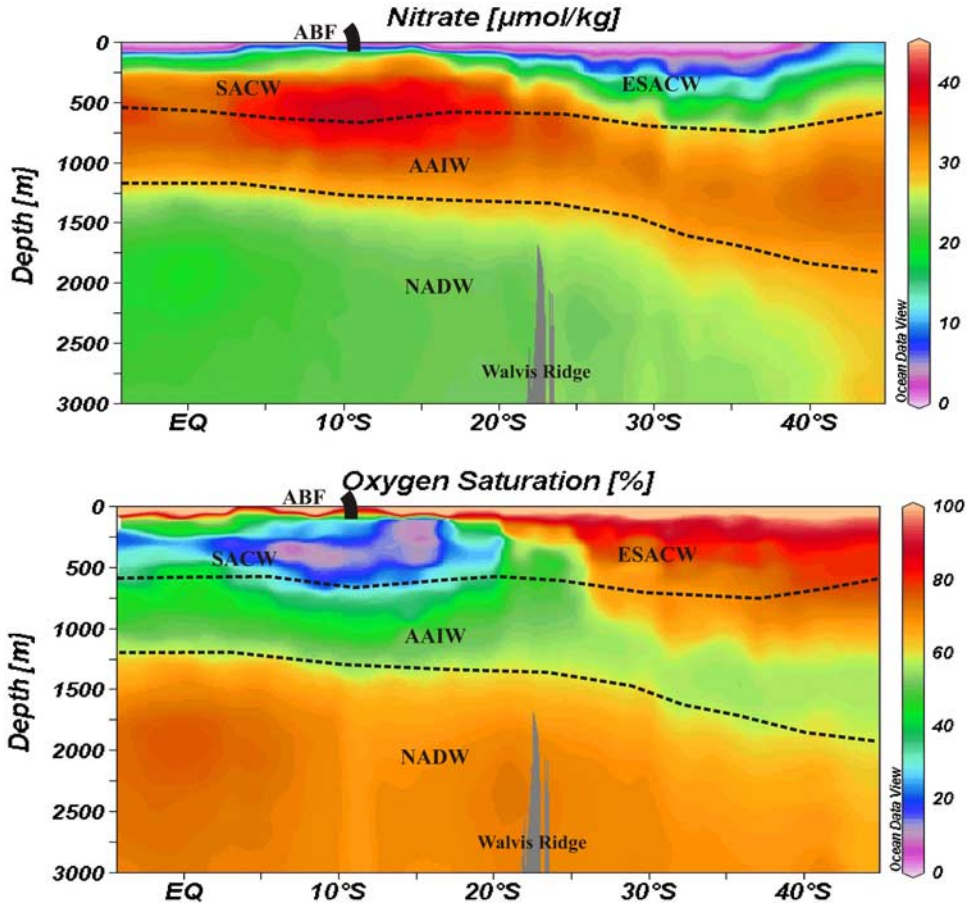

Figure 3. Nitrate and oxygen concentrations of the water masses (WOCE data, A13 profile). ABF, Angola Benguela Front; SACW, South Atlantic Central Water; ESACW, Eastern South Atlantic Central Water; AAIW, Antarctic Intermediate Water; NADW, North Atlantic Deep Water.

model was proposed for the BUS by *Hart and Currie* [1960] and henceforth adopted by numerous authors [*Bang*, 1971; *Shannon*, 1985; *Barange and Pillar*, 1992; *Giraudeau and Bailey*, 1995; *Summerhayes et al.*, 1995]. Maximum wind stress takes place 250 km offshore Namibia. This distance coincides roughly with the location of the shelf break. At the shelf edge, Ekman pumping of subsurface waters results from the conjunction of these topographical and atmospheric specificities. *Barange and Pillar* [1992] emphasized that the existence of these two cells is determined by the strength of the driving winds. In periods of high wind speed, the offshore cell is active and filaments of highly productive waters extend far from the coast. We propose that cross shore partitioning of the Namibian upwelling in two cells decouples nutrient dynamics over the plateau and beyond the shelf break. In accordance with water circulation models for two-celled upwellings [*Giraudeau et al.*, 2000; *Mollenhauer et al.*, 2002], we consider that heavy nitrates produced over the shelf by water column denitrification are re-utilized within the nearshore cell, then incorporated into planktonic biomass, but are scarcely advected beyond the shelf edge. Nitrate that upwells through the offshore cell stem mostly from subsurface waters surrounding the shelf break (Figure 4) and their isotopic signal is not influenced by processes occurring over the shelf.

5. Upwelling Dynamics and Nitrate Cycling in the Past

5.1. Wind Strength and SST Reconstructions

[21] Validation of the grain size variations as a wind strength proxy is given elsewhere [*Pichevin et al.*, 2005]. The wind strength reconstruction is in good agreement with previous studies located on Walvis Bay [*Little et al.*, 1997; *Shi et al.*, 2001; *Jahn et al.*, 2003]. Dust grain size is well correlated with SST variations of the upper slope core (Figure 5). We found a correlation coefficient of 0.61 between both records using Analyseries software [*Paillard et al.*, 1996]. Maximum upwelling intensity occurs during glacial periods and especially isotopic stages 3 and 4. Mismatches between past SSTs and the dust grain size are observed during early isotopic stage 6 and, according to *Schneider et al.* [1995], were ascribed to enhanced wind zonality which caused offshore displacement of the Benguela Current and, in turn, southward intrusion of warm Angola water in the Namibian upwelling area. This resulted in the decoupling of the

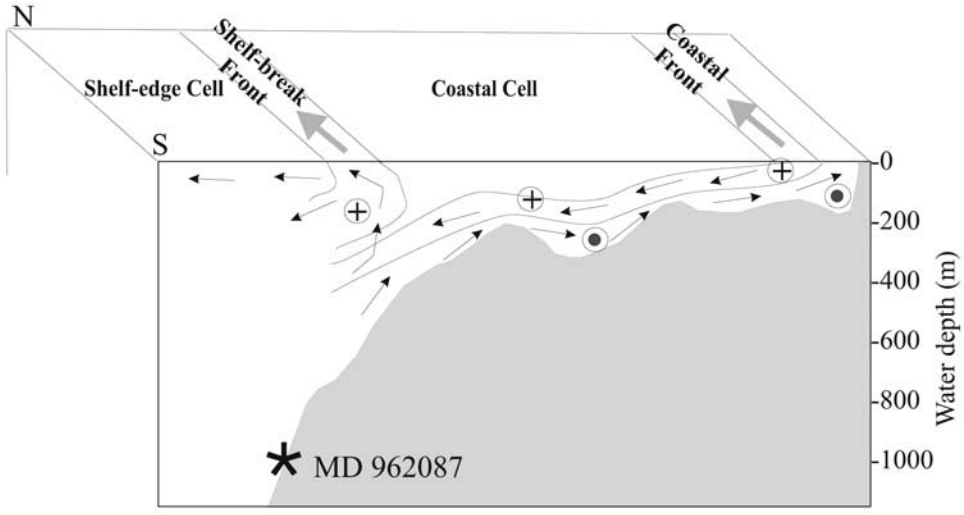

Figure 4. The two-cell structure of the upwelling. Encircled crosses are equatorward flows, encircled points are poleward flows. Sediments reaching the shallow core MD962087 mainly stem from the shelf. The accumulation rates are not shown for the Holocene because of sediment expansion at the top of the cores during retrieval which makes the values unrealistic.

coastal SSTs and upwelling intensity/productivity (Figure 4) during this period.

5.2. Organic Carbon Content and Accumulation Rate

[22] For hemipelagic deep-sea sediments, the organic carbon contents of the Lüderitz cores are surprisingly high (Figure 6) [*Bertrand et al.*, 2003]. TOC concentrations are typically higher during glacial periods, although this tendency is less obvious in the shallow cores. During marine isotopic stage (MIS) 6.6, organic carbon contents reach maximum values of 7.5, 12 and 17.5 wt.% at 3606, 2909 and 1028 m water depth, respectively. At all water depths, the lowest TOC contents occur during the full interglacial MIS 5.5., 1 and 7. Between 70 and 45 kyr BP, the upper slope core displays outstandingly high TOC values compared to the deep cores. The peak at 45 kyr seems partly correlated with the particularly low SST and intense wind strength prevailing during this interval.

[23] The calculated MARCorg show consistently strong similarities with the organic carbon contents. However, the peaks at 180 and 45 kyr appear significantly attenuated when expressed as accumulation rate rather than fraction of the bulk sediment. Thus the average MARCorg on the lower slope are equivalently high during the last two glacial periods and low during the interglacial periods. MIS 7 show extremely low MARCorg on both the upper and the lower slope. Organic carbon accumulation remains higher during MIS 6 compared to MIS 2, 3 and 4, in the shallow core,

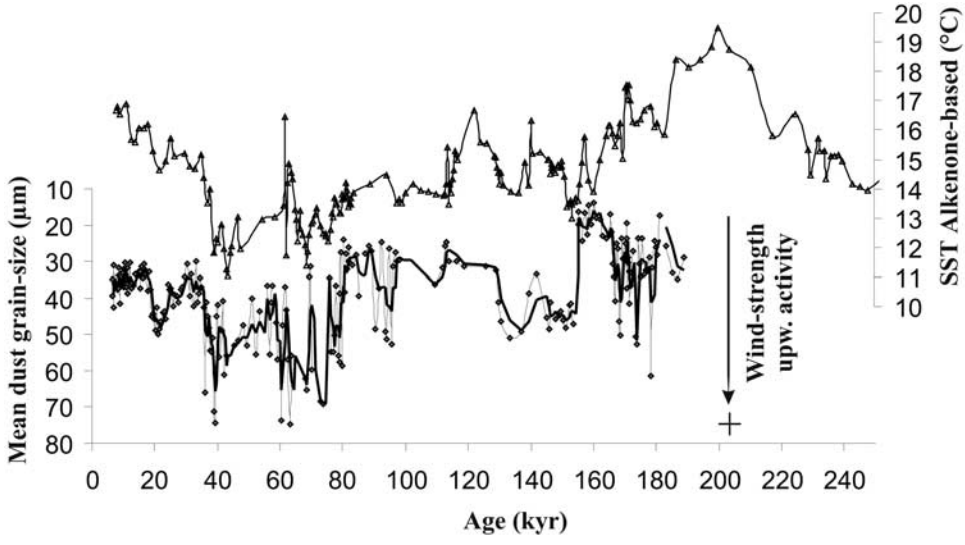

Figure 5. Dust grain size variations compared to SSTs changes in core MD962087.

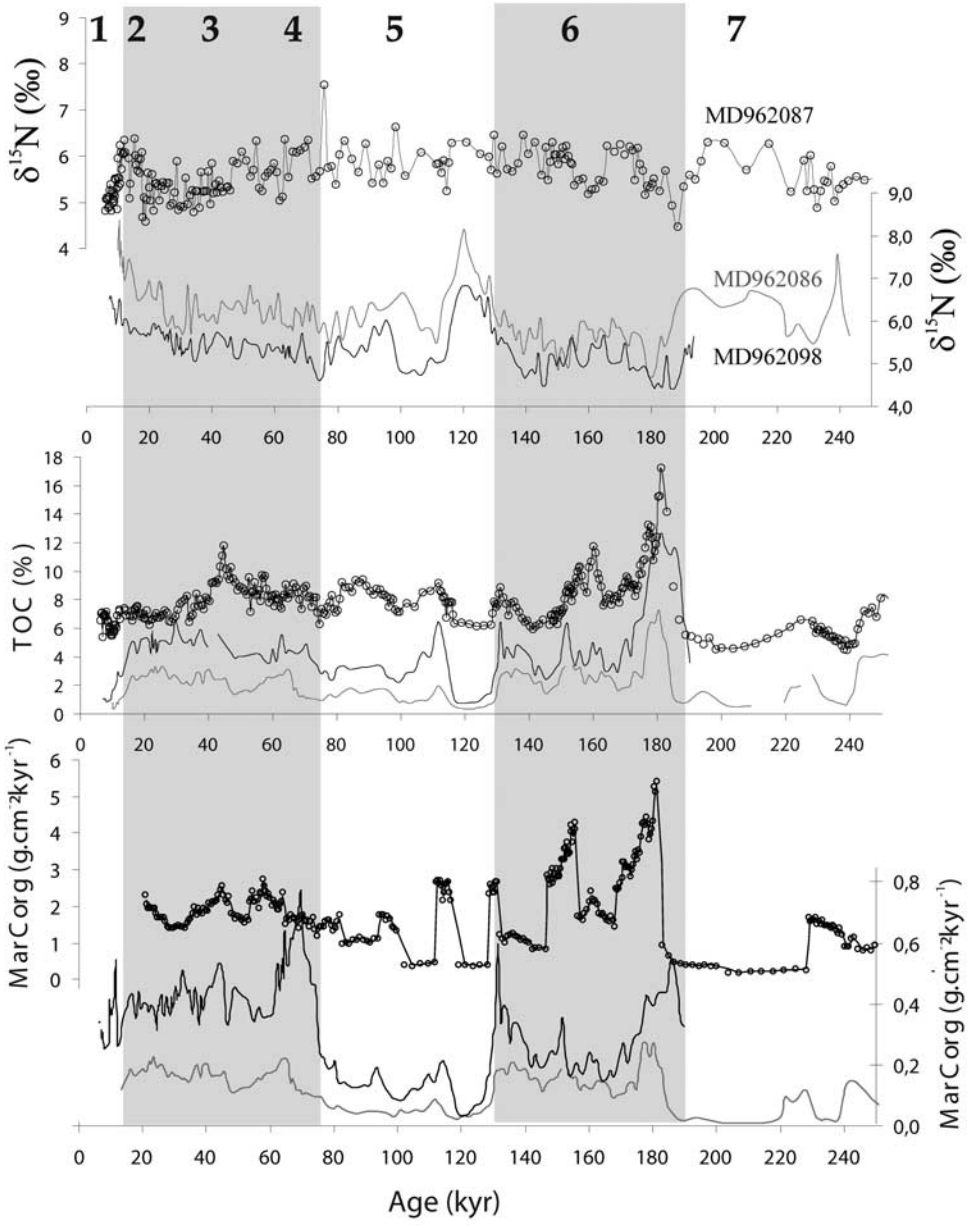

Figure 6. Organic carbon mass accumulation rates (MAPCorg), organic carbon contents (TOC), and nitrogen isotope signal ($\delta^{15}N$) of MD962087, MD962098, and MD962086. The accumulation rates are not shown for the Holocene because sediment expansion at the top of the cores during retrieval makes the values unrealistic. Glacial periods are indicated by gray shaded areas.

testifying for enhanced paleoproductivity over, and exported fluxes to, the upper slope during glacial MIS 6.

5.3. Nitrogen Isotope Signals

[24] The most striking feature displayed by the $\delta^{15}N$ data is the strong dissimilarity between upper and lower slope records (Figure 6). Albeit age models are based on few control points (20) and hence, are relatively imprecise for resolving suborbital variability, the $\delta^{15}N$ signals from the deep sites covary closely and demonstrate clear glacial-interglacial variations. Conversely, the upper slope $\delta^{15}N$ record shows comparatively high frequency, low amplitude variability without clear orbital cyclicity. Because of these differences, we discuss the deep and shallow sites separately.

5.3.1. Lower Slope

[25] The $\delta^{15}N$ signals vary between 4.7 and 8.2‰ in the deepest core and from 4.4 to 6.8‰ in the intermediate core. Broadly, sedimentary organic nitrogen is enriched in ^{15}N during warm periods, especially full interglacials, and depleted in ^{15}N during glacials. The nitrogen isotopic composition shows a weak negative correlation with the TOC records. By virtue of this inverse relationship, *Bertrand et al.* [2003] interpreted the $\delta^{15}N$ signal of

MD962086 as representing past surface nitrate utilization, lower values indicating lower nitrate utilization by primary producers during periods of high rate of nutrient supply and associated productivity. The same interpretation was put forward by *Holmes et al.* [1999, 2002, 2003] both in the modern Benguela and ancient Angola systems. Compared to the deepest core record, the $\delta^{15}N$ signal of MD962098 is consistently lighter by almost 1‰. The $\delta^{15}N$ signals increase with increasing distance from the coast, hence, from the emerging source of new nutrients. This pattern is consistent with the abovementioned ''utilization scenario'' proposed for the modern BUS.

5.3.2. Upper Slope

[26] The 100-kyr climate cyclicity is not recorded in the $\delta^{15}N$ signal of the nearshore core. The $\delta^{15}N$ values range approximately between 4.5 and 6.5‰. This range is comparable with that of the intermediate core. Assuming Rayleigh fractionation kinetics, this would suggest that, on average, past nutrient utilization was similar in the surface waters overlying both locations despite MD962087 being much closer to the coast. Under a continuous upwelling cell, if the ''utilization scenario'' were applicable, the $\delta^{15}N$ values on the upper slope would be expected to covary with the lower slope records, over a consistently lower range of values. Instead, both the variations and the range of the $\delta^{15}N$ values recorded in MD962087 imply a decoupling in the nutrient dynamics between the lower and upper slope locations. Alternatively, the signal of MD962087 has been altered by other biochemical processes than those likely to have affected the deeper cores.

6. Implications

6.1. Explaining the Upper Slope $\delta^{15}N$ Signal

[27] Differences between upper (1000 m) and lower (>2900 m water depth) slope $\delta^{15}N$ signals can hardly be due to biogeochemical reactions (such as OM degradation, diagenesis or denitrification) acting with variable intensity depending on the water depth:

[28] 1. More than 90% of settling OM is degraded between the surface and 1000 m water depth [*Suess*, 1980]. OM decay is thus negligible below this depth and can hardly involve any noticeable deviation of the $\delta^{15}N$ ratio between upper and lower cores.

[29] 2. Sedimentary denitrification, although implying nitrogen isotopes fractionation, results in an isotope effect close to zero because the nitrate used to remineralize the OM is almost completely consumed in the sediment [*Brandes and Devol*, 1997; *Sigman et al.*, 2001, 2003].

[30] 3. Incubation experiments [*Lehmann et al.*, 2003], sediment trap [*Saino and Hattori*, 1980; *Altabet*, 1991; *Altabet et al.*, 1999a] and sediment core studies [*Freudenthal et al.*, 2001], both in marine and lacustrine environments, give equivocal results concerning the isotope effect induced by the early diagenetic decay of OM. Sedimentary OM may undergo either enrichment or depletion in ^{15}N whether microbial activity develops under oxic or anoxic conditions [*Lehmann et al.*, 2002]. On the Namibian slope, bottom waters are currently oxygenated and pore water oxygen is rapidly consumed in the first 15 mm below seafloor at any depth [*Hensen et al.*, 2000]. Besides changes in bottom water oxygenation which determines the ''sign'' of the fractionation (i.e., ^{15}N enrichment and depletion), the amount of degradable OM that reaches the seafloor may influence the intensity of the $\delta^{15}N$ shift [*Freudenthal et al.*, 2001]. TOC and MARCorg of the three cores covary roughly. This implies that OM fluxes (and the ensuing diagenesis) increase and decrease approximately in phase for the three sites [*Pichevin et al.*, 2004].

[31] 4. Finally, terrigenous and inorganic nitrogen contents of the Lüderitz slope sediments are negligible, as the OM is mainly of marine origin [*Pichevin et al.*, 2004], and the N contents converge toward 0 for 0% TOC (Figure 7).

[32] The upper slope is supplied by organic particles originating from the overlying waters and, for a large part, from the outer shelf [*Giraudeau et al.*, 2000]. When discussing today's nitrate cycling in the BUS, we assumed that distinct $\delta^{15}N$ distribution pattern between slope and shelf surface sediments was likely due to the partitioning of the upwelling in two cells. We suggest that the decoupling of surface and subsurface water dynamics between nearshore and offshore upwelling cells largely contributes to the inconsistencies observed between the upper slope $\delta^{15}N$ record and the deeper ones. Upper slope $\delta^{15}N$ records is assumed to mostly reflect processes occurring in the nearshore cell whereas the lower slope records witness N cycling within the offshore cell.

[33] Excluding isotopic substages 5.3, 5.5 and MIS 7, TOC contents and accumulation rates are consistently very high on the upper slope, indicating highly productive conditions. In order to sustain such high productivity, nutrient requirements of the phytoplankton have to be covered. This implies efficient nitrate supply to the photic zone. The narrow amplitude of the $\delta^{15}N$ variations recorded in the upper slope sediments likely results from the fact that, even in periods of relatively weak winds and relaxed upwelling dynamics, nitrate was never severely depleted over the shelf. Limited OM accumulation on the upper slope during the last interglacial, compared to MIS 2, has been attributed to reduced exportation in context of high sea level stand, rather than decreasing paleoproduction [*Mollenhauer et al.*, 2002]. Thus TOC variations in MD962087 are more likely caused by shifts in sedimentation than by drastic changes in nitrate availability and attendant productivity. Perennially consistent nearshore upwelling enables marine nitrogen repletion of surface waters and may explain the low amplitude changes of the N isotopic ratio in MD962087 and its mean value close to 5.5‰.

[34] This situation is in clear contradiction with present, short term studies based on shallow trap sediments, which show that $\delta^{15}N$ and productivity are highly variable and seasonally driven by atmospheric and coastal water dynamics [*Romero et al.*, 2002; *Holmes et al.*, 2003, and references therein]. Hitherto, few data existed for the Namibian shelf and upper slope area. Further understanding of marine nitrogen cycling and hindcasting of paleoproductivity variations in the nearshore cell require closer scrutiny

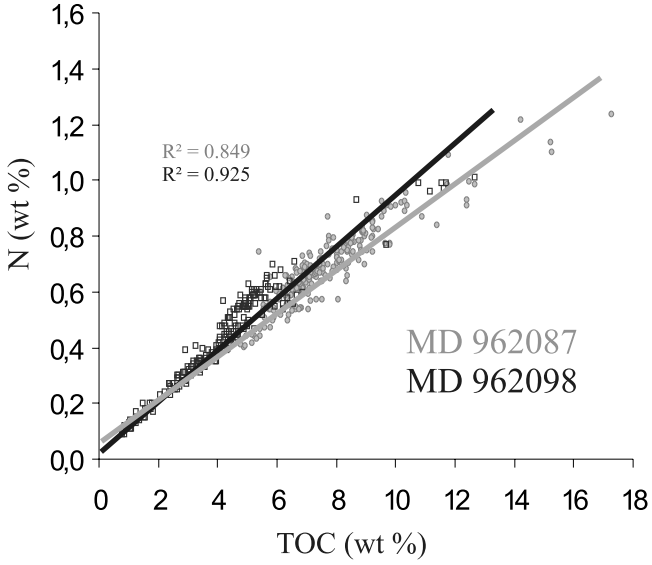

Figure 7. Organic carbon (TOC) versus nitrogen contents (N) in the sediments of MD962098 and MD972087.

through numerous $\delta^{15}N$ and TOC measurements of sediment cores, trap and water samples.

6.2. Reconstruction of Nitrate Utilization in the Deep Sites

[35] In upwelling regions, it is widely believed that productivity is chiefly driven by wind strength. This was often shown in the west African coast over seasonal to pluriannual timescales [e.g., *Holmes et al.*, 1998, 2002, 2003; *Giraudeau et al.*, 2000; *Romero et al.*, 2002]. Schematically, as SET wind stress increases, upwelling of subsurface waters accelerates, nutrient supply to the photic zone increases and primary production is not limited by nutrient availability. As a consequence, relative nutrient utilization diminishes. In such a context, proxies for upwelling dynamics, nutrient availability and productivity vary closely in tandem with interannual (El Niño/La Niña years) [*Altabet*, 2001] or seasonal cyclicities [*Holmes et al.*, 2002; *Romero et al.*, 2002]. Yet, such straightforward, causal relationship between upwelling activity (in physical terms) and paleoproductivity has never been demonstrated on geological timescales in the BUS, nor challenged.

[36] The $\delta^{15}N$ is not a proxy for nutrient supply or productivity, but for relative nitrate utilization as emphasized by *Altabet* [2001]. However, once productivity and utilization changes are assessed, NO_3 supply can be inferred. Using $\delta^{15}N$ records, we calculated the apparent relative utilization in the two deep cores, assuming Raleigh fractionation kinetics [*Altabet and Francois*, 1994], in order to determine whether or not past nitrate availability and utilization mirror changes in offshore upwelling intensity (given by the wind strength proxy).

[37] Variations of the unutilized fraction of nitrate (f) and TOC records from the deeper cores are compared with the wind strength signal (Figure 8). Broadly, TOC and *F* vary in tandem, which gives insights into NO_3 availability changes. Nevertheless, fluctuation of nutrient supply and (un)utilization is largely independent of wind forcing over the last 200 kyr as demonstrated by very low correlation coefficient (constantly <0.1, calculated using Analyseries [*Paillard et al.*, 1996]) between the wind strength proxy and both the $\delta^{15}N$ and *F* from the deeper cores. *Berger et al.* [2002] stress the point that, in eastern boundary current regions, upwelling-induced productivity depends on the wind stress, but also on the nutrient content of thermocline waters. In order to explain the lack of correlation between upwelling intensity and the other parameters we adduce the possibility that thermocline water fertility has changed over glacial-interglacial timescales, decoupling atmospheric forcing from NO_3 supply and productivity. TOC versus estimated relative nitrate utilization is plotted on Figure 9. Correlation between both parameters is weak, and values for full interglacial periods (namely the Holocene, Eemian and MIS 7.5) are invariably and clearly above the regression line: here, estimates of relative N utilization are greater than expected in case $\delta^{15}N$ faithfully represents relative nitrate utilization alone.

[38] This evidence points to variations in the (1) nitrate content or/and (2) isotopic ratio of upwelled waters as well as (3) potential changes in thermocline water sources, as additional factors controlling N inventory and paleoproductivity in the BUS (see below).

6.3. Imprint of Global Ocean Changes in Middepth Nitrate $\delta^{15}N$?

[39] According to *Shannon* [1985] waters that upwell on the Namibian shelf are Eastern South Atlantic Central Waters (ESACW, Figure 3) and stem from 50 to 300 m water depth, whereas the Antarctic Intermediate Water (AAIW) lies at 600 m water depth. The central water found in the tropical southeastern Atlantic is formed in large part by Indian Central Water brought into the Atlantic Ocean in the form of Agulhas rings and filaments [*Sprintall and Tomczak*, 1993]. This implies that South African upwelling cells are principally supplied in nitrate by waters coming from the southern South Atlantic and Indian Oceans. Agulhas waters partly originate from the Indian subtropical gyre (poor in nutrient) and to a lesser extent from the northern Indian Basin (Arabian Sea), both through the Mozambic Channel and with the poleward current, east of Madagascar [*Donohue and Toole*, 2003]. The northern sector of the Indian Ocean has long been recognized as one of the major denitrifying zones [*Naqvi*, 1987]. Episodes of enhanced N losses through denitrification in the Indian Basin occur during interglacial periods [*Altabet et al.*, 1995, 1999b] (Figure 10). Nevertheless, N budget in the Arabian Sea seems to respond to precessional (monsoon) forcing and, although the $\delta^{15}N$ signal shows clear increases during the two last deglacial transgressions, denitrification was not at maximum around 240 kyr BP [*Altabet et al.*, 1999b]. The Lüderitz and Arabian Sea $\delta^{15}N$ variations are reasonably in phase but their respective amplitude differ depending on the periods. *Pether* [1994] showed that the rate of Indian Ocean advection in the South Atlantic Ocean also changed over glacial/interglacial timescales. Owing to Southern Ocean warming and decreasing austral summer insolation, Agulhas advection in the Benguela region was enhanced during the

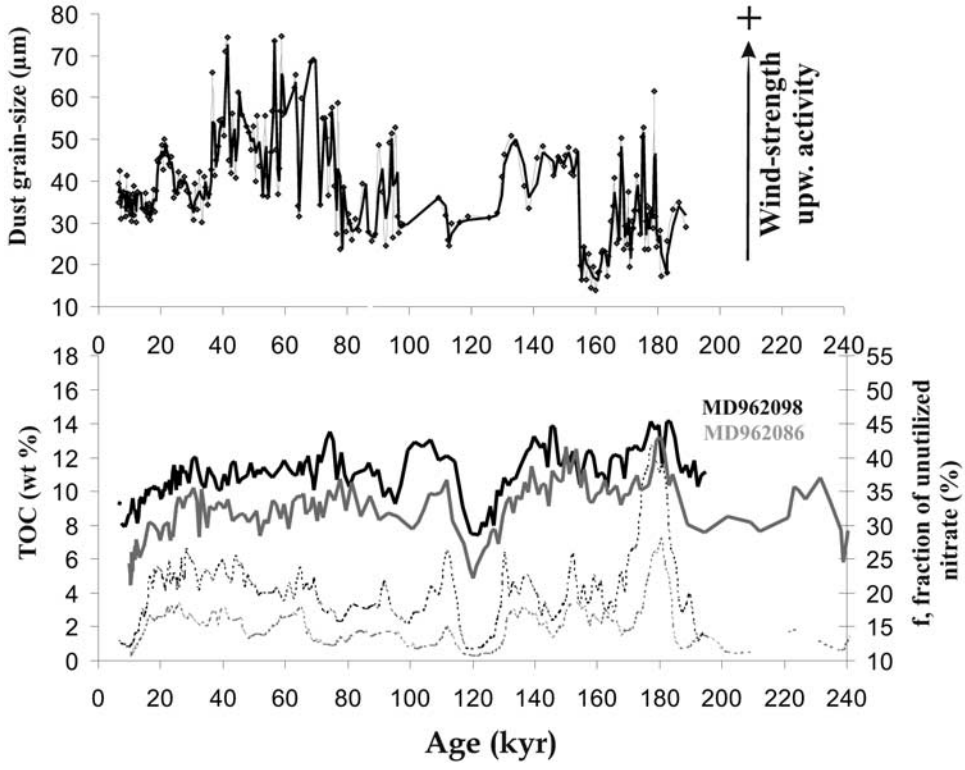

Figure 8. Unutilized fraction of nitrate (f, %) based on calculation of relative nitrate utilization (assuming Raleigh fractionation kinetic) for MD962086 and MD962098 compared to TOC and wind strength variations.

last deglaciations. Thus inflows of Indian water increased during transitions 1 and 2, arguably bringing an increased amount of nitrate depleted and/or ^{15}N enriched waters in the Benguela region toward deglaciations.

[40] Moreover, lower slope $\delta^{15}N$ records resemble those from further regions: recent nitrogen isotope measurements from the North Atlantic [*Martinez et al.*, 2000], South Atlantic [*Holmes et al.*, 1996], north Indian [*Altabet et al.*, 1999b], North Pacific [*Kiesnast et al*., 2002], and South Pacific oceans [*Ganeshram et al.*, 1999], invariably show low $\delta^{15}N$ values during glacials and exceptionally high sedimentary $\delta^{15}N$ during transitions and the following climatic optima [*Galbraith et al.*, 2004]. This common pattern, either concurrent or unrelated to local paleoproductivity changes, and observed in scattered sites from both OMZs and nondenitrifying zones, points to global changes in nitrate inventory between cold and warm stages. A growing body of evidence indicates that, over glacial-interglacial cycles, global ocean balance between N fixation and denitrification swung, probably impacting atmospheric CO_2 [*Ganeshram et al.*, 1995, 2000; *Altabet et al.*, 1999b] through alternatively reduced and invigorated biological pump. Increased water column denitrification in area adjoining OMZs was assumed to cause reductions in global ocean NO_3^- inventory during interglacial periods [e.g., *McElroy*, 1983]. We propose that the lower slope records are also partly driven by global ocean changes in middepth nitrate concentration and/or $\delta^{15}N$, which are in turn controlled by globally increased denitrification upon

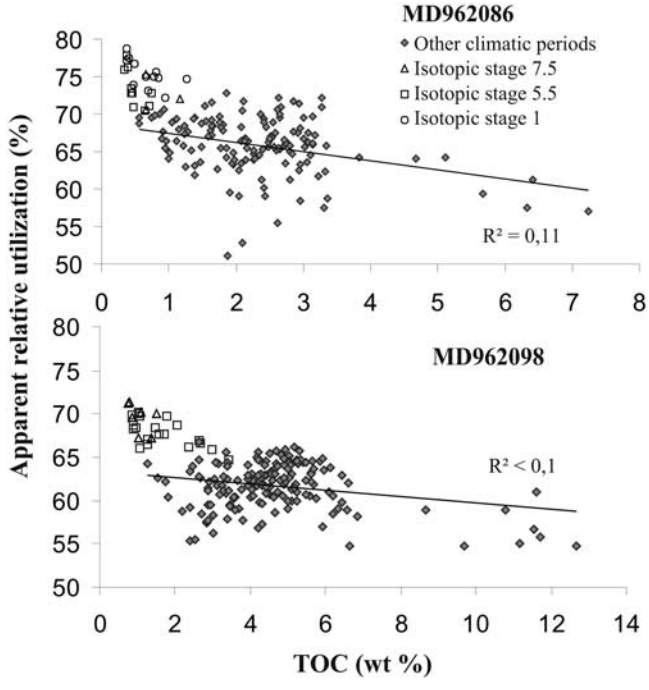

Figure 9. TOC versus relative nitrate utilization (%). Full interglacial values do not follow the tendency.

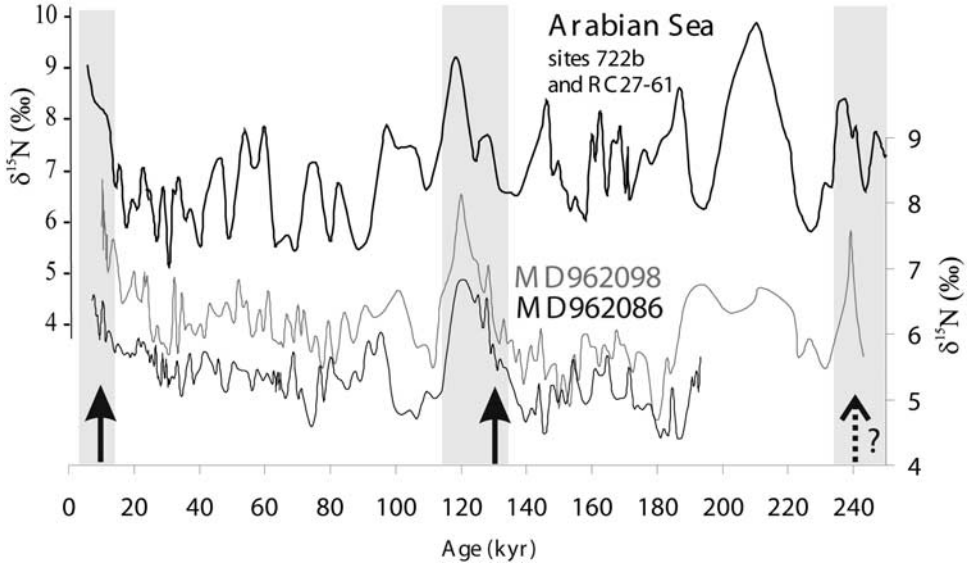

Figure 10. Nitrogen isotope signal of MD962098 and MD962086 compared with the Arabian Sea records, site 722b and RC2761 [*Altabet et al.*, 1999b]. Black arrows correspond to periods of enhanced Aguhlas water advection in the Benguela region [after *Pether*, 1994].

deglaciations. Nevertheless, this scenario is in contradiction with the fact that the upper slope $\delta^{15}N$ signal remains almost unchanged through time, but patterns of N cycling in the nearshore cell remains to be clarified.

[41] On the basis of the above inferences, we propose that impoverishment of the ESACW in nitrate toward deglaciations due to (1) enhanced denitrification in the world's OMZs, and particularly in the Indian Ocean, combined with (2) massive Agulhas water inflow in the Benguela during Terminations, plausibly explain both the $\delta^{15}N$ peaks and productivity minima recorded in the Namibian slope sediments around 10, 120 and 240 kyr BP, as well as the glacial-interglacial variability of the lower slope $\delta^{15}N$.

7. Conclusions

[42] In this work, we attempted to give a clear picture of present and past marine nitrogen budget in the Benguela upwelling system (BUS). First, major processes involved in nitrate cycling in the area today were examined on the basis of both previous studies and new, unpublished data of surface sediment $\delta^{15}N$. Glacial-interglacial variations of the upwelling activity, $\delta^{15}N$ and paleoproductivity signals were then studied in three sediments cores distributed from the upper to the lower continental slope off Lüderitz (25°6S).

[43] The lower slope cores display low $\delta^{15}N$ during cold periods and high $\delta^{15}N$ during climatic optima, akin to many other records from the world ocean, whereas the upper slope core displays a high-frequency, low-amplitude $\delta^{15}N$ signal without obvious glacial-interglacial variability. This dissimilarity results from the segregation of the upwelling structure in two cells, decoupling nutrient dynamics of the shelf from those beyond the shelf edge.

[44] For the deep cores, comparisons between N isotopic signals and indicators of paleoproductivity (TOC) and upwelling intensity (SSTs and dust grain size) revealed that, over Milankovitch cycles, nitrate delivery to the photic zone and attendant productivity were controlled by the nutrient richness of the South Atlantic Central Water, (depending in turn on Aguhlas water inflow and denitrification at a global scale), rather than by atmospheric forcing. In addition, we propose that the $\delta^{15}N$ signals of the deep cores do not only mirror changes in relative nitrate utilization, as it seems the case over annual timescales, but are also driven by global ocean changes in middepth nitrate $\delta^{15}N$.

[45] **Acknowledgments.** Financial support was provided by the ECLIPSE (CNRS) and GDR "Marges" (TFE) programs. The cores were retrieved during NAUSICAA cruise (IMAGE II) with the R/V *Marion Dufresne*. In this regard, we are grateful to IPEV and Yvon Balut. We particularly acknowledge J. Villanueva for giving us the liberty of publishing the SSTs estimates. We thank T. Ivanochko and an anonymous reviewer for valuable and thoughtful comments.

References

Altabet, M. A. (1991), Nitrogen isotopic evidence for the source and transformation of sinking particles in the open ocean, *Abstr. Pap. Am. Chem. Soc.*, *201*, 41.

Altabet, M. A. (2001), Nitrogen isotopic evidence for micronutrient control of fractional NO_3^- utilization in the equatorial Pacific, *Limnol. Oceanogr.*, *46*, 368–380.

Altabet, M. A., and R. Francois (1994), Sedimentary nitrogen isotopic ratio as a recorder for surface ocean nitrate utilization, *Global Biogeochem. Cycles*, *8*, 103–116.

Altabet, M. A., R. Francois, D. W. Murray, and W. L. Prell (1995), Climate related variations in denitrification in the Arabian Sea from sediment 15N/14N ratios, *Nature*, *373*, 506–509.

Altabet, M. A., C. Pilskaln, R. Thunell, C. Pride, D. Sigman, F. Chavez, and R. Francois

(1999a), The nitrogen isotope biogeochemistry of sinking particles from the margin of the eastern North Pacific, *Deep Sea Res., Part I*, *46*, 655–679.

Altabet, M. A., D. W. Murray, and W. L. Prell (1999b), Climatically linked oscillations in Arabian Sea denitrification over the past 1 m.y.: Implications for the marine N cycle, *Paleoceanography*, *14*, 732–743.

Bang, N. D. (1971), The Southern Benguela region in February 1966. Part II. Bathythermography and air-sea interactions, *Deep Sea Res.*, *18*, 209–224.

Barange, M., and S. C. Pillar (1992), Cross-shelf circulation, zonation and maintenance mechanisms of Nyctiphanes-Capensis and Euphausia-Hanseni (Euphausiacea) in the northern Benguela upwelling system, *Cont. Shelf Res.*, *12*, 1027–1042.

Berger, W. H., C. B. Lange, and G. Wefer (2002), Upwelling history of the Benguela-Namibia system: A synthesis of leg 175 results, *Proc. Ocean Drill. Program, Sci. Results*, *175*, 1–103.

Bertrand, P., T. F. Pedersen, P. Martinez, S. Calvert, and G. Shimmield (2000), Sea level impact on nutrient cycling in coastal upwelling areas during deglaciation: Evidence from nitrogen isotopes, *Global Biogeochem. Cycles*, *14*, 341–355.

Bertrand, P., et al. (2003), Organic-rich sediments in ventilated deep-sea environments: Relationship to climate, sea level, and trophic changes, *J. Geophys. Res.*, *108*(C2), 3045, doi:10.1029/2000JC000327.

Brandes, J. A., and A. H. Devol (1997), Isotopic fractionation of oxygen and nitrogen in coastal marine sediments, *Geochim. Cosmochim. Acta*, *61*, 1793–1801.

Brandes, J. A., and A. H. Devol (2002), A global marine-fixed nitrogen isotopic budget: Implications for Holocene nitrogen cycling, *Global Biogeochem. Cycles*, *16*(4), 1120, doi:10.1029/2001GB001856.

Brandes, J. A., A. H. Devol, T. Yoshinari, D. A. Jayakumar, and S. W. A. Naqvi (1998), Isotopic composition of nitrate in the central Arabian Sea and eastern tropical North Pacific: A tracer for mixing and nitrogen cycles, *Limnol. Oceanogr.*, *43*, 1680–1689.

Carr, M. E. (2002), Estimation of potential productivity in eastern boundary currents using remote sensing, *Deep Sea Res. Part II*, *49*, 59–80.

Chapman, P., and L. V. Shannon (1987), Seasonality in the oxygen minimum layers at the extremities of the Benguela system, *S. Afr. J. Mar. Sci.*, *5*, 51–62.

Conkright, M., S. Levitus, T. O'Brien, T. P. Boyer, J. Antonov, and C. Stephens (1998), *World Ocean Atlas 1998 Data Set Documentation* [CD-ROM], *Tech. Rep. 15*, Natl. Oceanogr. Data Cent., Silver Spring, Md.

Dittmar, T., and M. Birkicht (2001), Regeneration of nutrients in the northern Benguela upwelling and the Angola-Benguela Front areas, *S. Afr. J. Sci.*, *97*, 239–246.

Donohue, K. A., and J. M. Toole (2003), A near-synoptic survey of the southwest Indian Ocean, *Deep Sea Res. Part II*, *50*, 1893–1931.

Francois, R., M. P. Bacon, M. A. Altabet, and L. D. Labeyrie (1993), Glacial interglacial changes in sediment rain rate in the southwest Indian sector of Subantarctic waters as recorded by Th-230, Pa-231, U, and Delta-N-15, *Paleoceanography*, *8*, 611–629.

Freudenthal, T., T. Wagner, F. Wenzhofer, M. Zabel, and G. Wefer (2001), Early diagenesis of organic matter from sediments of the eastern subtropical Atlantic: Evidence from stable nitrogen and carbon isotopes, *Geochim. Cosmochim. Acta*, *65*, 1795–1808.

Galbraith, E. D., M. Kienast, T. F. Pedersen, and S. E. Calvert (2004), Glacial-interglacial modulation of the marine nitrogen cycle by high-latitude O_2 supply to the global thermocline, *Paleoceanography*, *19*, PA4007, doi:10.1029/2003PA001000.

Ganeshram, R. S., T. F. Pedersen, S. E. Calvert, and J. W. Murray (1995), Large changes in oceanic nutrient inventories from glacial to interglacial periods, *Nature*, *376*, 755–758.

Ganeshram, R. S., S. E. Calvert, T. F. Pedersen, and G. L. Cowie (1999), Factors controlling the burial of organic carbon in laminated and bioturbated sediments off NW Mexico: Implications for hydrocarbon preservation, *Geochim. Cosmochim. Acta*, *63*, 1723–1734.

Ganeshram, R. S., T. F. Pedersen, S. E. Calvert, G. W. McNeill, and M. R. Fontugne (2000), Glacial-interglacial variability in denitrification in the world's oceans: Causes and consequences, *Paleoceanography*, *15*, 361–376.

Giraudeau, J., and G. W. Bailey (1995), Spatial dynamics of coccolithophore communities during an upwelling event in the Southern Benguela System, *Cont. Shelf Res.*, *15*, 1825–1852.

Giraudeau, J., G. W. Bailey, and C. Pujol (2000), A high-resolution time-series analyses of particle fluxes in the Northern Benguela coastal upwelling system: Carbonate record of changes in biogenic production and particle transfer processes, *Deep Sea Res. Part II*, *47*, 1999–2028.

Gordon, A. L., K. T. Bosley, and F. Aikman (1995), Tropical Atlantic water within the Benguela Upwelling System at 27 degrees S, *Deep Sea Res. Part I*, *42*, 1–12.

Hart, T. J., and R. I. Currie (1960), The Benguela Current, *Disc. Rep.*, *31*, 123–298.

Hay, W. W., and J. C. Brock (1992), Temporal variation in intensity of upwelling of southwest Africa, in *Upwelling Systems: Evolution Since the Early Miocene*, *Geol. Soc. Spec. Publ.*, vol. 63, edited by C. P. Summerhayes et al., pp. 463–497, Geol. Soc., London.

Hensen, C., M. Zabel, and H. D. Schulz (2000), A comparison of benthic nutrient fluxes from deep-sea sediments off Namibia and Argentina, *Deep Sea Res. Part II*, *47*, 2029–2050.

Holmes, E., G. Lavik, G. Fischer, M. Segl, G. Ruhland, and G. Wefer (2002), Seasonal variability of delta N-15 in sinking particles in the Benguela upwelling region, *Deep Sea Res. Part I*, *49*, 377–394.

Holmes, M. E., P. J. Muller, R. R. Schneider, M. Segl, J. Patzold, and G. Wefer (1996), Stable nitrogen isotopes in Angola Basin surface sediments, *Mar. Geol.*, *134*, 1–12.

Holmes, M. E., P. J. Muller, R. R. Schneider, M. Segl, and G. Wefer (1998), Spatial variations in euphotic zone nitrate utilization based on delta N-15 in surface sediments, *Geo-Mar. Lett.*, *18*, 58–65.

Holmes, M. E., C. Eichner, U. Struck, and G. Wefer (1999), Reconstruction of surface ocean nitrate utilization using stable nitrogen isotopes in sinking particles and sediments, in *Use of Proxies in Paleoceanography: Examples From the South Atlantic*, edited by G. Fischer and G. Wefer, pp. 447–468, Springer, New York.

Holmes, M. E., G. Lavik, G. Fisher, and G. Wefer (2003), Nitrogen isotopes in sinking particles and surface sediments in the central and southern Atlantic, in *The South Atlantic in the Late Quaternary: Reconstruction of Material Budgets and Current Systems*, edited by G. Wefer, S. Mulitzas, and V. Ratmeyer, pp. 143–165, Springer, New York.

Imbrie, J., J. D. Hays, D. G. Martinson, A. McIntyre, A. C. Mix, J. J. Morley, N. G. Pisias, W. L. Prell, and N. J. Shackleton (1984), The orbital theory of Pleistocene climate: Support from a revised chronology of the marine $\delta^{18}O$ record, in *Milankovitch and Climate*, edited by A. Berger et al., pp. 269–305, D. Reidel, Norwell, Mass.

Jahn, B., B. Donner, P. J. Müller, U. Rohl, R. R. Schneider, and G. Wefer (2003), Pleistocene variations in dust input and marine productivity in the northern Benguela Current: Evidence of evolution of global glacial-interglacial cycles, *Palaeogeogr. Palaeoclimatol. Palaeoecol.*, *193*, 515–533.

Kirst, G. J., R. R. Schneider, P. J. Müller, I. von Storch, and G. Wefer (1999), Late Quaternary temperature variability in the Benguela Current System derived from alkenones, *Quat. Res.*, *52*, 92–103.

Largier, J., and A. J. Boyd (2001), Drifter observations of surface water transport in the Benguela Current during winter 1999, *S. Afr. J. Sci.*, *97*, 223–229.

Lass, H. U., M. Schmidt, V. Mohrholz, and G. Nausch (2000), Hydrographic and current measurements in the area of the Angola-Benguela front, *J. Phys. Oceanogr.*, *30*, 2589–2609.

Lavik, G. (2001), Nitrogen isotopes of sinking matter and sediments in the South Atlantic, 174 pp., Ber. aus dem Fachber. Geowiss. der Univ. Bremen, Bremen.

Lehmann, M. F., S. M. Bernasconi, A. Barbieri, and J. A. McKenzie (2002), Preservation of organic matter and alteration of its carbon and nitrogen isotope composition during simulated and in situ early sedimentary diagenesis, *Geochim. Cosmochim. Acta*, *66*, 3573–3584.

Lehmann, M. F., P. Reichert, S. M. Bernasconi, A. Barbieri, and J. A. McKenzie (2003), Modelling nitrogen and oxygen isotope fractionation during denitrification in a lacustrine redox-transition zone, *Geochim. Cosmochim. Acta*, *67*, 2529–2542.

Little, M. G., R. R. Schneider, D. Kroon, B. Price, C. P. Summerhayes, and M. Segl (1997), Trade wind forcing of upwelling, seasonality, and Heinrich events as a response to sub-Milankovitch climate variability, *Paleoceanography*, *12*, 568–576.

Lutjeharms, J. R. E., and J. M. Meeuwis (1987), The extent and variability of South-East Atlantic upwelling, *S. Afr. J. Mar. Sci.*, *5*, 51–62.

Mariotti, A., F. Mariotti, M.-L. Champigny, N. Amaner, and A. Moyse (1982), Nitrogen isotope fractionation associated with nitrate reductase activity and uptake of NO_3^- by pearl millet, *Plant Physiol.*, *69*, 880–884.

Martinez, P., P. Bertrand, S. E. Calvert, T. F. Pedersen, G. B. Shimmield, E. Lallier-Vergès, and M. R. Fontugne (2000), Spatial variations in nutrient utilization, production and diagenesis in the sediments of a coastal upwelling regime (NW Africa): Implications for the paleoceanographic record, *J. Mar. Res.*, *58*, 809–835.

McElroy, M. B. (1983), Marine biological controls on atmospheric CO_2 and climate, *Nature*, *302*, 328–329.

Minagawa, M., and E. Wada (1984), Stepwise enrichment of ^{15}N along the food chains: Further evidence and the relation between

$\delta^{15}N$ and animal age, *Geochim. Cosmochim. Acta*, *48*, 1135–1140.

Mohrholz, V., M. Schmidt, and J. R. E. Lutjeharms (2001), The hydrography and dynamics of the Angola-Benguela Frontal Zone and environment in April 1999, *S. Afr. J. Sci.*, *97*, 199–208.

Mollenhauer, G., R. R. Schneider, P. J. Müller, V. Spieß, and G. Wefer (2002), Glacial/interglacial variability in the Benguela upwelling system: Spatial distribution and budgets of organic carbon accumulation, *Global Biogeochem. Cycles*, *16*(4), 1134, doi:10.1029/2001GB001488.

Montoya, J. P., and J. J. McCarthy (1995), Isotopic fractionation during nitrate uptake by phytoplankton grown in continuous-culture, *J. Plankton Res.*, *17*, 439–464.

Morse, J. W., and K. C. Emeis (1992), Carbon/sulphur/iron relationships in upwelling sediments, in *Upwelling Systems: Evolution Since the Early Miocene*, edited by C. P. Summerhayes et al., *Geol. Soc. Spec. Publ.*, 64, pp. 247–255.

Naqvi, S. W. A. (1987), Some aspects of the oxygen deficient conditions and denitrification in the Arabian Sea, *J. Mar. Res.*, *45*, 1049–1972.

Paillard, D., L. Labeyrie, and P. Yiou (1996), Macintosh program performs time-series analysis, *Eos Trans. AGU*, *77*, 379.

Peterson, R. G., and L. Stramma (1991), Upper-level circulation in the South Atlantic Ocean, *Progr. Oceanogr.*, *26*, 1–73.

Pether, J. (1994), Molluscan evidence for enhanced deglacial advection of Agulhas Water in the Benguela Current, off southwestern Africa, *Palaeogeogr. Palaeoclimatol. Palaeoecol.*, *111*, 99–117.

Pichevin, L., P. Bertrand, M. Boussafir, and J.-R. Disnar (2004), Organic matter accumulation and preservation controls in a deep-sea modern environment: An example from Namibian Slope sediments, *Org. Geochem.*, *35*, 543–559.

Pichevin, L., M. Cremer, J. Giraudeau, and P. Bertrand (2005), A 190 kyr record of lithogenic grain-size on the Namibian slope: Forging a tight link between past wind-strength and coastal upwelling dynamics, *Mar. Geol.*, in press.

Prahl, F. G., L. A. Muehlhausen, and D. L. Zahnle (1988), Further evaluation of long-chain alkenones as indicators of paleoceanographic conditions, *Geochim. Cosmochim. Acta*, *52*, 2303–2310.

Romero, O., B. Boeckel, B. Donner, G. Lavik, G. Fischer, and G. Wefer (2002), Seasonal productivity dynamics in the pelagic central Benguela System inferred from the flux of carbonate and silicate organisms, *J. Mar. Sys.*, *37*, 259–278.

Saino, T., and A. Hattori (1980), ^{15}N natural abundance in oceanic suspended particulate matter, *Nature*, *283*, 752–754.

Schneider, R. R., P. J. Müller, and G. Ruhland (1995), Late Quaternary surface circulation in the east equatorial South Atlantic: Evidence from alkenone sea-surface temperatures, *Paleoceanography*, *10*, 197–219.

Schulz, H. D., A. Dahmke, U. Schinzel, K. Wallmann, and M. Zabel (1994), Early diagenetic processes, fluxes, and reaction-rates in sediments of the South Atlantic, *Geochim. Cosmochim. Acta*, *58*, 2041–2060.

Shannon, L. V. (1985), The Benguela ecosystem. Part I. Evolution of the Benguela, physical features and processes, *Oceanogr. Mar. Biol. Annu. Rev.*, *23*, 105–182.

Shannon, L. V., and G. Nelson (1996), The Benguela: Large scale features and processes and system variability, in *The South Atlantic Ocean, Present and Past Circulation*, edited by G. Wefer et al., pp. 163–210, Springer, New York.

Shi, N., R. Schneider, H. J. Beug, and L. M. Dupont (2001), Southeast trade wind variations during the last 135 kyr: Evidence from pollen spectra in eastern South Atlantic sediments, *Earth Planet. Sci. Lett.*, *187*, 311–321.

Sigman, D. M., M. A. Altabet, R. Michener, D. C. McCorkle, B. Fry, and R. M. Holmes (1997), Natural abundance-level measurement of the nitrogen isotopic composition of oceanic nitrate: An adaptation of the ammonia diffusion method, *Mar. Chem.*, *57*, 227–242.

Sigman, D. M., K. L. Casciotti, M. Andreani, C. Barford, M. Galanter, and J. K. Bohlke (2001), A bacterial method for the nitrogen isotopic analysis of nitrate in seawater and freshwater, *Anal. Chem.*, *73*, 4145–4153.

Sigman, D. M., R. Robinson, A. N. Knapp, A. van Geen, D. C. McCorkle, J. A. Brandes, and R. C. Thunell (2003), Distinguishing between water column and sedimentary denitrification in the Santa Barbara Basin using the stable isotopes of nitrate, *Geochem. Geophys. Geosyst.*, *4*(5), 1040, doi:10.1029/2002GC000384.

Smith, R. L. (1995), The physical processes of coastal ocean upwelling systems, in *Upwelling in the Ocean: Modern Processes and Ancient Records*, edited by C. P. Summerhayes et al., pp. 39–64, John Wiley, Hoboken, N. J.

Sprintall, J., and M. Tomczak (1993), On the formation of central water and thermocline ventilation in the Southern Hemisphere, *Deep Sea Res. Part I*, *40*, 827–848.

Stuiver, M., P. J. Reimer, E. Bard, J. W. Beck, G. S. Burr, K. A. Hughen, B. Kromer, G. McCormac, J. Van der Plicht, and M. Spurk (1998), INTCAL98 radiocarbon age calibration, 24,000–0 cal BP, *Radiocarbon*, *40*, 1041–1083.

Suess, E. (1980), Particulate organic carbon flux in the ocean, *Nature*, *288*, 260–263.

Summerhayes, C. P., D. Kroon, A. Rosell-Mele, R. W. Jordan, H.-J. Schrader, R. Hearn, J. Villanueva, J. O. Grimalt, and G. Eglington (1995), Variability in the Benguela Current upwelling system over the past 70,000 years, *Progr. Oceanogr.*, *35*, 207–251.

Sweeney, R. E., and I. R. Kapland (1980), Natural abundance of ^{15}N as a source indicator for near-shore marine sedimentary and dissolved nitrogen, *Mar. Chem.*, *9*, 81–94.

Tyrrell, T., and M. I. Lucas (2002), Geochemical evidence of denitrification in the Benguela upwelling system, *Cont. Shelf Res.*, *22*, 2497–2511.

Villanueva, J., and J. O. Grimalt (1997), Gas chromatographic tuning of the $U(k')37$ paleothermometer, *Anal. Chem.*, *69*, 3329–3332.

Wada, E. (1980), Nitrogen isotope fractionation and its significance in biogeochemical processes occurring in marine environments, in *Isotope Marine Chemistry*, edited by E. D. Goldberg, Y. Horibe, and K. Surahashi, pp. 375–398, Ushida Rokakuho, Tokyo.

P. Bertrand, J. Giraudeau, P. Martinez, and R. Schneider, Département de Géologie et Océanographie, Université Bordeaux I, UMR-CNRS 5805, F-33405 Talence Cedex, France.

K. Emeis, Institute of Biogeochemistry and Marine Chemistry, University of Hamburg, Bundesstrasse 53, Hamburg D-20146, Germany.

L. Pichevin, CEREGE, Europole Méditerranéen de l'Arbois, UMR 6635, BP 80, F-13545 Aix en Provence Cedex 04, France. (pichevin@cerege.fr)